IEEE Access
Multidisciplinary | Rapid Review | Open Access Journal

Received February 7, 2021, accepted February 24, 2021, date of publication February 26, 2021, date of current version April 2, 2021.

Digital Object Identifier 10.1109/ACCESS.2021.3062465

Research on the Gate Oxide Layer Aging Trend of Power Electronic Device

GUOQING XU[1], (Senior Member, IEEE), LINGFENG SHAO[1], WEIWEI WEI[1], YANHUI ZHANG[2], AND XUECHENG SUN[1]

[1]School of Mechatronic Engineering and Automation, Shanghai University, Shanghai 200444, China
[2]Shenzhen Institute of Advanced Technology, Chinese Academy of Sciences (CAS), Shenzhen 518055, China

Corresponding author: Lingfeng Shao (lfshao@shu.edu.cn)

This work was supported in part by the National Key Research and Development Program of China under Grant 2016YFB0100700 and Grant 2018YFB0104803.

ABSTRACT The introduction of fully electric vehicles (FEVs) into the mainstream has raised concerns about the reliability of their electronic components such as Insulated Gate Bipolar Translator (IGBT). At present, only the transient thermal resistance curve in the datasheet and the initial thermal model of the experimental test are used to evaluate the life of the IGBT module, while it is well known that IGBT parameters are affected by its degree of aging. Thus, the development of research for the aging process of IGBT is of key importance. The aging process of IGBT is proposed to be a gradual aging process, verified by the accelerated aging experiment. Firstly, the mechanism between the relevant aging parameters and the degree of IGBT aging is studied in this paper. Secondly, the switching parameters in different degrees of aging are measured and compared by accelerated experiments. Finally, the stepwise linear regression algorithm is used to screen parameters and the Mann-Kendall test method is used to analyze the IGBT aging process curve. The results show that the aging process of IGBT is gradual, and the aging process model of IGBT is finally established. On this basis, the remaining using life of IGBT can be accurately measured.

INDEX TERMS Insulated gate bipolar transistor, accelerated aging experiment, stepwise regression algorithm, Mann-Kendall test method.

I. INTRODUCTION

Insulated Gate Bipolar Transistor (IGBT), a power electronic device, is widely used in electric vehicles, new energy generation, and rail transit. With the development of power devices towards the trend of high voltage class, high power density, and high load operation, the reliability of power electronic devices has become a focus issue [1]–[5]. The aging of IGBT is a time-dependent random process, which is influenced by the accumulation of internal fatigue damage and the external operating environment. The main failure forms of IGBT include chip failure and package failure, among which chip failure is more difficult to monitor online. IGBT chip failures include radiation damage and gate oxide layer aging [6], among which radiation damage is mainly caused by cosmic rays, nuclear radiation, and other external factors.

Power electronic equipment is less affected by radiation under normal working conditions, so the aging of IGBT chips is mainly caused by gate oxide layer aging. The gate oxide layer of IGBT is a SiO_2 thin film connecting the electrical insulation of the gate-pole and emitter. Because the oxygen layer is very thin and easy to break down, so it is one of the weak links in the IGBT chip.

The reliability analysis of IGBT based on gate-oxygen aging is the focus of this paper. Gate-oxygen aging is an evolutionary process of occurrence, development, and complete failure, and IGBT can continue to work for a while before the gate oxide layer brokes down. Therefore, if this potential change can be detected before complete failure, catastrophic failure can be avoided.

To evaluate the gate oxide aging curve of IGBT and find the IGBT modules with defects in the converter in time, scholars at home and abroad have conducted extensive research on the aging monitoring of IGBT modules. A lot of research has been done on the determination and extraction of characteristic parameters [7]–[11], including collector-emitter saturation voltage drop [12], gate-emitter voltage [13], gate-emitter threshold voltage [14], short-circuit current [15], [16], gate current I_C [17], junction temperature T_j, etc.

The associate editor coordinating the review of this manuscript and approving it for publication was Ali Raza.

In literature 16, using V_{ce} measurement as a real-time supervision method is evaluated by using aging test results obtained on insulated gate bipolar transistor (IGBT) modules stressed by power cycling [18].In literature 17, the thermal stress on bond wires of aged insulated gate bipolar transistor modules under short-circuit conditions has been studied for different solder delamination levels. Amir proposes that a short-circuit current can be used to characterize the degree of aging [19]. Wang proposed to monitor the junction temperature of IGBT in real-time and detect the degree of aging through the junction temperature by placing two thermal sensors for each switch at the interface between the baseplate of an IGBT module and the cold plate [20]. And the duration of the Miller plateau during the IGBT turn-on transition is proposed as an online precursor indicating two dominant types of failures by Dr. Liu [21]. Reference 20 directly evaluates reliability by using a large number of collected failure time data, which can also obtain relatively accurate evaluation results [22].

Although the problem of IGBT monitoring has been addressed in several studies [22]–[25], the single aging parameter is very unstable for the study of the aging trend of IGBT, which is easily affected by external factors. The innovation of this paper lies in:

1. It is proposed that the highest junction temperature of IGBT power devices occurs during the switching process, and the traditional temperature-sensitive electrical parameters (TSEP) can also be considered as aging-parameters. These aging-parameters are affected by junction temperature, collector current, and degree of aging, and can be used for IGBT aging prediction and health management systems.

2. Besides, by comparing the changing trend of aging parameters with aging evolution, it can be found that the aging process of IGBT is gradual.

The second chapter mainly introduces the aging mechanism of IGBT and demonstrates the feasibility of accelerating the experiment. In chapter III, the effect of portal oxygen aging on switching process parameters is studied. In chapter IV, some algorithms are used to screen aging-parameters and demonstrate the aging process, including stepwise regression algorithm and Mann-Kendall trend testing method. In chapter V, this paper introduces the platform and design of an accelerated aging experiment. In chapter VI, the experimental results are analyzed and demonstrated that the aging of IGBT power devices is a progressive aging process. There is a summary in Chapter VII.

II. FAILURE MECHANISM OF IGBT

A. THE FAILURE PROCESS OF IGBT

IGBT devices can be summarized from manufacturing, delivery, using, and failure by bathtub curve, which is mainly composed of three parts, as shown in FIG. 1.

Stage 1: Early Failure rate (EFR); The high failure rate of devices is mainly due to manufacturing defects and low factory standards.

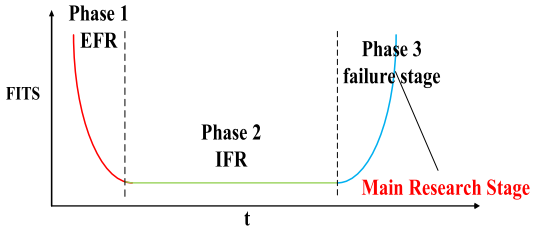

FIGURE 1. Bath curve of the device reliability.

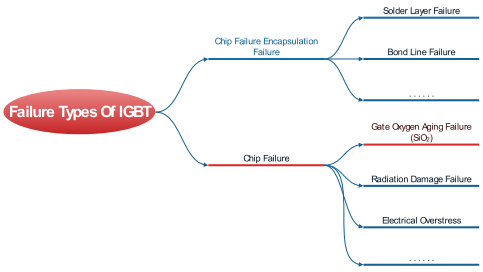

FIGURE 2. Failure types of IGBT.

Stage 2: Intrinsic Failure rate (IFR); The device has a low and stable failure rate after the initial phase.

Stage 3: In the failure stage; The device is more prone to failure, which is mainly caused by the aging of the gate oxide layer.

Among them, the third stage is the most complex and meaningful research process. To detect the relationship between the degree of portal oxygen aging of IGBT and working time, accelerated aging of IGBT devices is required in this experiment, and the degree of aging is mainly analyzed through power cycle [26] or thermal cycle experiment [27], [28]. The project team chose to apply a continuous voltage to the gate poles of IGBT to simulate the process of its gating oxygen aging and verified that gate-oxygen aging of IGBT is a progressive aging process through a large number of experimental data.

B. MECHANISM OF IGBT GATE-OXYGEN AGING FAILURE

The third stage of IGBT aging includes package aging and chip aging. Among them, chip failure includes gate-oxygen aging, radiation damage, etc., [9]. The aging of IGBT is mainly caused by the aging of the gate oxide layer, which includes time-dependent dielectric breakdown (TDDB) and hot-carrier injection (CHI). The aging pattern of IGBT is shown in FIG. 2.

TDDB, the gate voltage is lower than intrinsic breakdown field strength and does not cause the intrinsic breakdown, while after a certain period, the gate oxide layer breakdown occurred. TDDB is one of the main factors affecting device life and system reliability. When a constant voltage is applied to the polar oxide layer in the IGBT, the continuous aging of the oxide (SIO_2) will create a conductive path within it, and the device will lose control and be broken down. The process deteriorates rapidly with the decrease of the thickness of IGBT gate oxide.

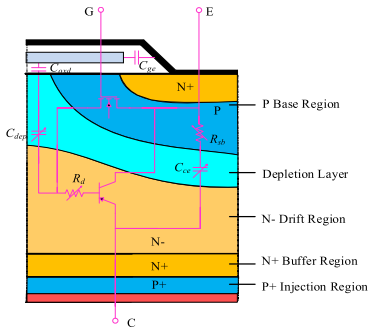

FIGURE 3. Internal structure diagram of IGBT chip cell.

TDDB is generally divided into two development stages [29]. In the first stage, the trap charge density of the new IGBT oxygen layer is very low, but the tunneling current will create neutral traps in the dielectric with the following effects:

1. The charge will be captured by the existing trap, and its external characteristics are shown as the threshold voltage and leakage current of the device change;
2. New traps are created in the oxide layer.

The aging of the device induced by hot carrier injection (CHI) is caused by high-energy electrons and hole injection gate oxide layer. During the injection process, the interface state and trap charge of the oxide layer will be generated, resulting in damage to the oxide layer. The probability of the hot carrier injection depends directly on the channel length, oxide layer thickness, and operating voltage of the device. When energy obtained by the leakage current flowing through the channel is higher than the lattice temperature, hot carriers will be generated. For very small devices, even at low voltages, a strong electric field can be generated, which can easily lead to the emergence of hot carriers. These hot carriers have enough energy to be ejected into the gate oxide layer, resulting in charge traps and interfacial states. The latter will change the external characteristics of IGBT (such as threshold voltage, transconductance, and leakage current, etc.), and eventually, causing device failure with the increase of damage degree [30].

III. EFFECT OF IGBT GATE OXIDE LAYER AGING ON SWITCHING CHARACTERISTICS

In the process of gate oxide layer aging of IGBT, interelectrode capacitors, such as C_{gc} and C_{ge}, will change with the aging degree, which will lead to the change of voltage and current parameters, and then lead to the change of relevant switching characteristic parameters. Therefore, appropriate switching characteristic parameters can be used to characterize the aging degree of IGBT and reveal its aging curve. The internal structure of the IGBT chip cell is divided into four layers of PNPN structure, as shown in FIG. 3.

Gate-collector capacitance (Miller capacitance) C_{gc} is a series of gate-oxide capacitance C_{oxd} and depletion layer capacitance C_{dep} below the gate oxide. C_{gc} can be calculated

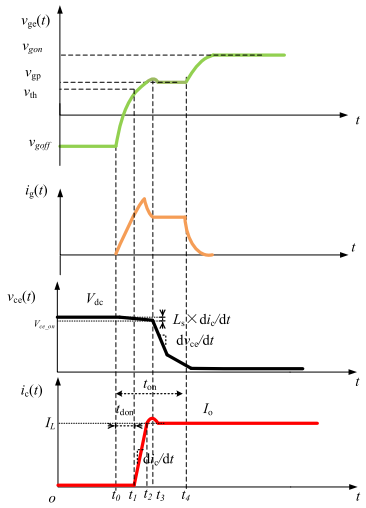

FIGURE 4. Calibration and definition of relevant parameters in turn-on process of IGBT.

using the following formula:

$$C_{gc} = \frac{C_{oxd} C_{dep}}{C_{oxd} + C_{dep}} \tag{1}$$

$$C_{oxd} = C_{ox} A \alpha_i \tag{2}$$

$$C_{dep} = A \sqrt{\frac{q \cdot N_n \cdot \varepsilon_{Si}}{2(U_{CE} - U_{CE(th)})}} \tag{3}$$

where Coxd represents the oxide layer capacitance, C_{ox} represents the oxide layer capacitance per unit area, and A represents the chip area. a_i represents the ratio of internal cellular area to total area.

With the aging and evolution of IGBT, the gate-oxide layer thickness (pole spacing) became thinner [9], [35], which leads to the increase of C_{oxd}. According to formula (1) - (3), with the IGBT gate oxygen aging, the Miller capacitance C_{gc} also changes, which means that the aging-parameters related to Miller capacitance can be used to characterize the degree of IGBT gate oxide layer aging. Therefore, this paper studies its correlation according to the relationship between the measured aging-parameters and the degree of aging

A. ANALYSIS OF IGBT TURN-ON PROCESS

The turn-on process of IGBT is mainly composed of four stages. Parameters such as turn-on delay time, current rising time, and turn-on loss can be extracted. The states of IGBT in each stage are shown in FIG. 4 respectively. [V_{ge}(gate-emitter voltage), i_g(gate current), V_{ce}(gate-emitter voltage), i_c(collector current)]

Phase I (t_0~t_1): Turn-on delay time t_{don}. The voltage of the IGBT gate changes from V_{goff} to V_{gon}, and the drive power supplies charge IGBT's input capacitance C_{ies} through the drive resistance, where $C_{ies} = C_{gc} + C_{ge}$.

The time of duration from t_0 to t_1 is considered as the turn-on delay time and can be expressed in Equation 4.

$$t_{\text{don}} = \Delta t_1 = R_g \left(C_{\text{gc}} + C_{\text{ge}}\right) \ln \frac{V_{\text{gon}} - V_{\text{goff}}}{V_{\text{gon}} - V_{\text{th}}} \tag{4}$$

where R_g is gate resistance, V_{gon} is gate pole on-state voltage, V_{goff} is gate pole off-state voltage, V_{th} is the turn-on threshold voltage.

Phase II (t_1~t_2): Collector current rising time t_{ri}. In the second stage, the gate continues to charge, and as the gate-emitter voltage V_{ge} is higher than the turn-on threshold voltage V_{th}, the load current I_C flows to the IGBT from the continuation diode.

Phase III (t_2~t_3): Miller platform time. When the collector current I_C reaches a certain value, it returns to I_L. Since IGBT works in the active region at this stage, the collector current I_C keeps a constant value, and the gate voltage is clamped at constant value V_{gp}, which is the miller platform at this stage. At this time, the gate current I_g is also maintained at a constant value, i.e.

$$I_g = \frac{V_{\text{gon}} - V_{gp}}{R_g} \tag{5}$$

Therefore, the gate current only charges the capacitor C_{gc}, and at the same time, the Collector emitter voltage V_{ce} begins to drop. This period is as follows:

$$t_{gp} = \frac{C_{GC\_AVG}(V_{CE} - V_{CE\_ON})}{I_g} \tag{6}$$

where C_{GC_AVG} is the average value of Miller capacitor C_{gc} in the third-stage, I_g is the charging current of the Miller capacitor.

Phase IV (t_3~t_4): Gate charging time. At t = t_3, the working point of IGBT enters the saturation region from the boundary of the active region, and the gate voltage breaks through the Miller platform to continue charging the input capacitor C_{ies}. At this stage, the collector-emitter voltage becomes the on-state voltage drop.

Research shows that when the IGBT's gate oxide layer is aged, the conductive path is formed inside the oxide layer, and a part of the charge will flow to the emitter through the gate oxide layer

In the fourth stage, the gate current I_g will decrease. According to Formula 6, with the decrease of I_g, time t_{gp} will increase, thereby increasing the voltage decreasing time t_{vf}, and slowing down the opening speed of IGBT, thus changing the opening characteristics of IGBT.

B. ANALYSIS OF IGBT TURN-OFF PROCESS

The turn-off process of IGBT can be divided into three stages for analysis. Parameters such as turn-off delay time, voltage fallen time, and turn-off loss can be extracted, as shown in Fig. 5.

Phase I (t_0~t_1): Turn-off delay time t_{doff}. The drive voltage changes rapidly when the gate drive sends out a turn-off signal; then, the drive current is established and discharged through the drive resistance, while the gate voltage V_{ge} drops and the collector current I_C keeps I_0 due to the inductive load. Finally, the gate voltage drops to the Miller platform voltage

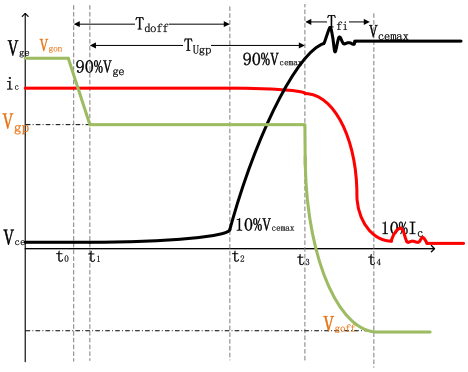

FIGURE 5. Calibration and definition of relevant parameters in turn-off process of IGBT.

V_{gp}. The duration is recorded as the turn-off delay time t_{doff}.

$$t_{\text{doff}} = R_{\text{g}}\left(C_{\text{ge}} + C_{\text{gc}}\right)\ln\left(\frac{V_{\text{gon}} - V_{\text{goff}}}{V_{\text{gp}} - V_{\text{goff}}}\right) + \frac{(V_{\text{gp}} - V_{\text{ce(sat)}})R_{\text{g}}C_{\text{gc,L}}}{V_{\text{gp}} - V_{\text{goff}}} \tag{7}$$

Phase II (t_1~t_2): Miller platform time. When the gate voltage is clamped on the Miller platform, the gate voltage is V_{gp}. In the case of the resistance-type drive circuit, the gate current I_g remains constant, i.e.

$$I_g = \frac{V_{goff} - V_{gp}}{R_g} \tag{8}$$

At this point, the gate current charges the Miller capacitor C_{gc}, and since the collector voltage V_{ce} is low, the C_{gc} remains unchanged. When V_{ce} reaches value of V_{ge}, the value of Miller capacitance C_{ge} decreases sharply. At this point, the collector-emitter voltage V_{ce} starts to rise rapidly, and the voltage rising time is defined as:

$$t_{rv} = (V_{CE} - V_{gp}) * \frac{C_{GC}}{I_G} \tag{9}$$

Phase III (t_2~t_3): Current falling time. When the collector-emitter voltage V_{CE} of IGBT is equal to the bus voltage V_{DC}, the continuation diode is forward biased. Then the load current I_L begins to transfer from IGBT to the diode. The falling time of voltage and changing rate of voltage can be extracted.

Phase IV (t_3~t_4): Trailing current time. At t = t_3, the gate voltage V_{ge} continues to drop, and the collector current I_C also drops. Due to the bus voltage, the remaining carriers in the IGBT are slowly drawn away. Besides, the charges stored in IGBT are gradually compounded.

IV. ALGORITHM

A. PARAMETER SCREENING ALGORITHM BASED ON STEPWISE REGRESSION

The results show that there are a large number of switch characteristic parameters related to the degree of aging, but some of the parameters have strong coupling, and some of them are affected by other external interference factors. Therefore,

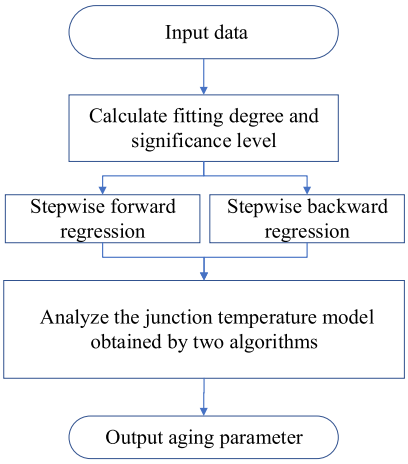

FIGURE 6. A flow chart of extraction of aging parameters based on stepwise regression.

this paper proposes a switching process parameter screening based on a stepwise regression algorithm, which can improve calculation speed by screening out the parameters independent of the degree of aging/weak coupling. The algorithm is divided into the following three steps, the main purpose is to eliminate insignificant variables, the flow chart is shown in Fig 6.

Step 1: Set the significance level F used to eliminate independent variables in advance, and establish the regression equation of all independent variables (Associated aging parameters: $X_1, X_2, \ldots, X_m$) to dependent variables (Y degree of aging). And F test is carried out on the regression coefficient ($b_1, b_2, \ldots, b_m$) of m independent variables in the equation, denoted as:$\{F_1{}^1, F_2{}^1 \ldots, F_m{}^1\}$, then take the minimum value $F_{k1}{}^1 = \min\{F_1{}^1, F_2{}^1 \ldots, F_m{}^1\}$; If $F_{k1}{}^1 > F$, then go to the next step; otherwise, remove $F_{k1}{}^1$ and repeat this step.

Step 2: Take the external independent variable and the degree of aging to establish the regression equation. If its significance is greater than F, the independent variable is added to the regression equation in Step 1; If not, enter Step 3.

Step 3: Output the regression equation and determine the aging parameters.

Through the above cycle, the regression equation is the optimal equation until the F value of the regression coefficient of each variable in the regression equation is greater than the critical value. This means that the coupling degree between relevant parameters extracted by this algorithm and the degree of aging is high enough. This improves the accuracy of the degree of aging analysis and reduces subsequent data processing time.

B. CURVE ANALYSIS OF AGING PROCESS BASED ON THE MANN-KENDALL TREND TEST

Due to encapsulation, the aging degree of IGBT cannot be directly observed. Therefore, in this paper, appropriate switching process parameters are selected as the main characteristic quantity to monitor the degree of IGBT aging, and high-dimensional data are mapped into two-dimensional space (aging parameter - aging time). Finally, the aging process is monitored by the algorithm. As a typical trend testing method, the Mann-Kendall trend testing method has been recommended by the World Meteorological Organization (WMO) and widely used. It has many advantages, such as no need to obey certain distribution, no interference from few outliers, a high degree of quantization, wide monitoring range, ease to calculate, and more suitable for order variables and type variables. For time series X with n samples, an order column is constructed:

$$S_k = \sum_{i=1}^{k} r_i, \quad k = 2, 3, \ldots, n \tag{10}$$

where r_i can be equal to:

$$r_i = \begin{cases} +1 & x_i > x_j \\ +0 & x_i \le x_j \end{cases} \quad j = 1, 2, \ldots, i \tag{11}$$

It can be seen that the order column S_k is the cumulative count of the number of values at that time i greater than that at time j. Define statistic UK_K under the assumption of random independence of time series:

$$UK_k = \frac{|S_k - E(S_k)|}{\sqrt{var(S_k)}}, \quad k = 1, 2, \ldots, n \tag{12}$$

where $UK_1 = 0$, $E(S_k)$, and $var(S_k)$ are the mean and variance of Sk.

The $x_1, x_2, \ldots, x_N$ are independent of each other and have the same continuous distribution. They can be calculated by the following formula 13:

$$\begin{cases} E(S_k) = \dfrac{k(k-1)}{4} \\ \mathrm{var}(S_k) = \dfrac{k(k-1)(2k+4)}{72} \end{cases} \quad k = 2, 3, \ldots, n \tag{13}$$

UF_k is the standard normal distribution. It is a statistical sequence calculated in chronological order ($x_1, x_2, \ldots, x_n$). Repeat the process in reverse chronological order ($x_n, x_{n-1}, \ldots, x_1$), while $UB_k = -UF_k$ (k = n, n-1 . . . 1), $UB_1 = 0$. According to the given significance level F and critical value u, the aging trend can be obtained through two statistics (UF_k, UB_k) and critical value u.

V. DESIGN OF AGING EXPERIMENT PLATFORM

A. DESIGN OF IGBT ACCELERATED AGING SCHEME

In this experiment, the IGBT (FF50R12RT4) modules with different degrees of aging are double-pulse tested to extract the parameters related to the degree of aging, and finally, the aging evolution process is studied. The research shows that gate oxide layer aging is caused by high voltage pressure, so high voltage can be used to simulate the aging process of the gate [31]–[34]. In this paper, a 75V DC voltage is applied to the gate-emitter of IGBT to simulate its aging process [31], [35]. The gate emitter bias was applied for 4 hours to achieve accelerated aging. Immediately after aging,

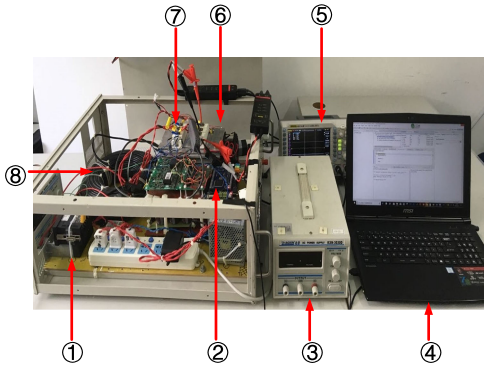

FIGURE 7. IGBT aging test platform.

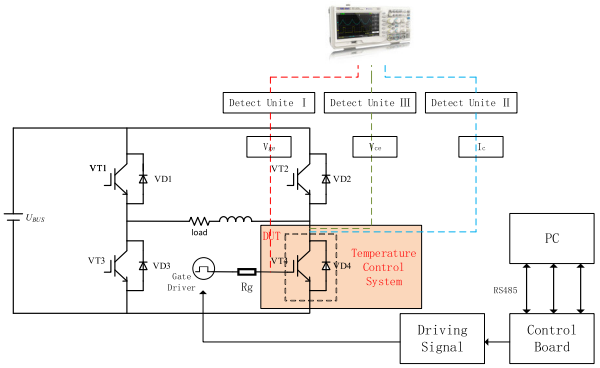

FIGURE 8. Test circuit for IGBT aging experiment.

a double-pulse test was performed on the power device. The total accelerated aging time was 20 hours, and then the data were recorded.

B. DESIGN OF THE MAIN CIRCUIT FOR AGING TEST

The experimental circuit is composed of DC power supply, IGBT, load and protective inductance, etc. It is mainly used to simulate the aging evolution process under working conditions. The experimental platform used in the laboratory is shown in FIG. 7, and the specific experimental circuit is shown in FIG. 8.

The experimental equipment in FIG. 7 is: (1) PTC (plate of temperature controller); (2) control board provides a control signal for the driver; (3) high power DC power supply (4) upper computer; (5) mixed-signal oscilloscope; (6) high voltage differential probe and high precision current probe; (7) cooling fan; (8) IGBT module to be tested; (9) inductive load.

PC, RS484, and control plate are used to conduct the double-pulse test on IGBT. During the test process, characteristic information such as gate voltage, collector current, and emitter voltage is extracted. Relevant characteristic information could be used to characterize the gate oxygen aging process of IGBT.

VI. EXPERIMENT AND SIMULATION

The MatLab 2016a and SPSS are used for data analysis, and Windows 10 system was used as the operating system.

TABLE 1. Model summary based on stepwise forward regression.

Model	R	R^2	Adjusted R^2	Error of standard estimate
1	.681[a]	.464	.354	5.55723
2	.680[b]	.463	.371	5.48471
3	0673[c]	.453	.377	5.45839
4	.642[d]	.412	.348	5.58101

a. predictive variable: (constant), t_{fv}, t_{rv}, t_{gp}, t_{fi}, t_{don}, t_{doff}, I_C
b. predictive variable: (constant), t_{fv}, t_{rv}, t_{gp}, t_{fi}, t_{doff}, I_C
c. predictive variable: (constant), t_{rv}, t_{gp}, t_{fi}, t_{doff}, I_C
d. predictive variable: (constant), t_{gp}, t_{fi}, t_{doff}, I_C

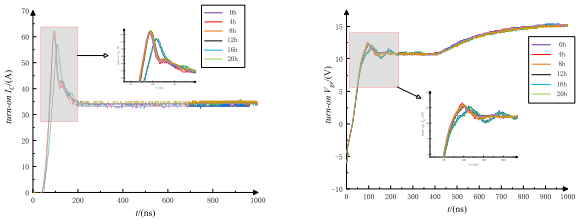

FIGURE 9. The curve of collector current and gate voltage during IGBT' turn-on process while $T_j = 30°C$, $I_C = 35A$.

By analyzing the data of the IGBT module after accelerated aging, the trend of IGBT gate oxygen aging can be found.

In this experiment, the aging parameters such as turn-off delay time, turn-on delay time, voltage rising time, miller voltage, and Miller platform time were extracted under different conditions (Aging time=0h\4h\...16h\20h; Collector current I_C = 10A\15A\...\35A\40A; Junction temperature T_j = 30°C\70°C). Where the room temperature is 30°C, and the IGBT condition is 70°C. This experiment was repeated 10 times, and the final average value was taken for the subsequent calculation. Since the relationship between aging-parameters and the degree of aging is similar at 30°C and 70°C, the filtered aging-parameters at 30°C are shown in Table 2, based on the stepwise regression algorithm. The above aging-parameters were tested by a stepwise regression algorithm, and the test results are shown in Tables 1 and 2. The aging model of IGBT is established based on the switching characteristic parameters, as shown in Equation 14. The turn-on process of IGBT under different degrees of aging (such as T_j = 30°C, I_C = 30A) is shown in FIG. 9. The turn-on process of IGBT under different degrees of aging (such as T_j = 70°C, I_C = 30A) is shown in FIG. 10. FIG. 11 shows the turn-off process of IGBT under different aging conditions (such as T_j = 30°C, I_C = 35A). FIG. 12 shows the turn-off process of IGBT under different aging conditions (such as T_j = 70°C, I_C = 35A). According to the model determined in Table 1 and Formula 14, the related aging parameters are tested by the Mann-Kendall test method. The trend test results of the aging-parameters and degree of aging based on the Mann-Kendall trend test method are shown in FIG. 13- FIG. 15.

$$Degree\ of\ Aging = f_1{}^*t_{doff} + f_2{}^*t_{gp} + f_3{}^*t_{fi} + k \qquad (14)$$

where each coefficient is corresponding to the B value in the above table, K is the constant value.

TABLE 2. Coefficient[a] based on stepwise forward regression.

Model		Unstandardized coefficient B	Unstandardized coefficient Standard error	Standardized coefficient Beta	t	Significance level
1	constant	-242.47	140.559		-1.725	.094
	I_C	.559	.331	.819	1.690	.100
	t_{doff}	.633	.339	.894	1.865	.071
	t_{gp}	-.088	.037	-.627	-2.412	.021
	t_{rv}	.125	.151	.327	.826	.414
	t_{fi}	-.043	.019	-.678	-2.196	.035
	t_{don}	.147	.484	.097	.304	.763
	t_{fv}	.021	.033	.187	.624	.537
2	constant	-218.73	115.355		-1.896	.066
	I_C	.553	.326	.810	1.696	.099
	t_{doff}	.603	.321	.852	1.880	.068
	t_{gp}	-.083	.033	-.594	-2.558	.015
	t_{rv}	.135	.146	.353	.926	.361
	t_{fi}	-.044	.019	-.703	-2.390	.022
	t_{fv}	.024	.030	.222	.809	.424
3	constant	-182.65	105.889		-1.725	.093
	I_C	.627	.312	.918	2.011	.052
	t_{doff}	.505	.295	.713	1.708	.096
	t_{gp}	-.085	.032	-.607	-2.635	.012
	t_{rv}	.199	.122	.521	1.637	.110
	t_{fi}	.053	.015	-.834	-3.411	.002
4	constant	-273.76	92.116		-2.972	.005
	I_C	.683	.317	1.000	2.158	.038
	t_{doff}	.808	.236	1.141	3.428	.002
	t_{gp}	-.086	.033	-.610	-2.590	.014
	t_{fi}	-.041	.014	-.656	-2.929	.006

a. dependent variable: Time

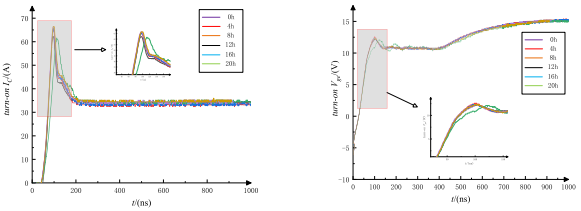

FIGURE 10. The curve of collector current and gate voltage during IGBT' turn-on process while $T_j = 70°C$, $I_C = 35A$.

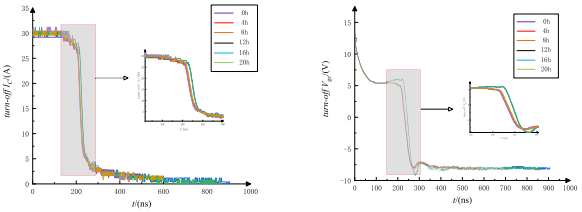

FIGURE 11. The curve of collector current and gate voltage during IGBT' turn-off process while $T_j = 30°C$, $I_C = 30A$.

As shown in Table 1 and Table 2, the aging-parameters such as turn-off delay time, current fallen time, and Miller platform time are closely related to aging evolution in the experiment, and the aging degree can even be calibrated with these aging-parameters.

In Figure 9-10, it can be found that during the turn-on process of IGBT, there is a small spike in the collector current rising, which is caused by the reverse recovery process of the continuation diode, leading to the continued increase of collector current. In the figure, the green curve is the turn-on process curve of IGBT after 20 hours of aging, and the purple curve is the turn-on process curve of healthy IGBT. It can be

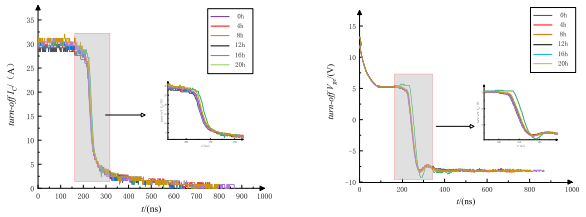

FIGURE 12. The curve of collector current and gate voltage during IGBT' turn-off process while $T_j = 70°C$, $I_C = 30A$.

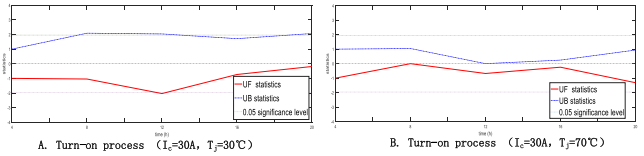

FIGURE 13. Trend analysis based on current fallen time while $I_C = 30A$.

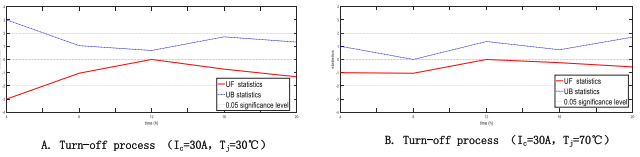

FIGURE 14. Trend analysis based on Miller platform time t_{gp} at turn-off process while $I_C = 30A$.

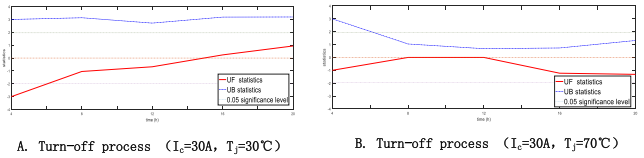

FIGURE 15. Trend analysis based on turn-off delay t_{doff} time while $I_C = 30A$.

seen that the turn-on period of IGBT increases with the aging evolution.

It can be seen from FIG. 11 and FIG. 12 that the collector current of IGBT decreases rapidly during the turn-off process. And there's the Miller platform phenomenon when the emitter voltage drops. This is because the Miller capacitance in IGBT increases with the evolution of gate-oxygen aging, which leads to longer turn-off delay time and longer duration of the riser platform. The green curve is the IGBT's turn-off process after 20 hours of aging, and the purple curve is the IGBT's turn-off process in the healthy state. It can be found that both the IGBT's turn-off process and the Miller platform duration are positively correlated with the degree of aging. Similarly, in the turn-off process of IGBT, the rate of the current decline is accelerated with the evolution of aging. In the left figure in Figure 11-12, the green curve is also the turn-off curve of IGBT after 20 hours of aging.

The above four pictures show that the parameters (turn-off delay time, current fallen time, Miller platform time) screened by stepwise regression algorithm are related to the degree of aging of IGBT and can be used for the analysis of the degree of aging.

As can be seen from FIG. 13-15, there is no intersection point between U_K and U_B, which means that the whole aging

process is a gradual change process. And there is no mutation point. Therefore, the aging process of IGBT and other power devices is a gradual aging process, which is proposed based on the stepwise regression algorithm and Mann-Kendall test method. This means that the aging process of devices such as IGBT can be calibrated by the aging parameters (turn-off delay time, turn-on delay time, Miller platform time).

VII. CONCLUSION

With the rapid development of electric vehicles, reliability problems of IGBT and other power semiconductor devices have become prominent. In this paper, it is revealed that the gate oxide capacitance decreases gradually with the evolution of aging, and the miller capacitance of IGBT increases according to the mechanism, which leads to the change of the external switching characteristics of IGBT (the switching process becomes longer).

Then the relevant characteristic parameters of IGBT after aging are obtained through experiments, and the aging trend is studied in this paper. The aging trend analysis of IGBT based on stepwise regression algorithm and Mann-Kendall trend test method is proposed. For the third stage in FIG.1, which is considered complex and difficult to analyze in previous studies, this paper proposed for the first time that the aging process could be characterized by aging parameters and that it is a progressive aging process. This indicates that in subsequent studies, the degree of aging of IGBT can be characterized with high precision by relevant aging parameters, and its residual life can also be measured. It can avoid the system collapse due to the complete failure of the device.

The main conclusions of this paper are as follows:

(1) The highest temperature of IGBT is in the switching process, that is, the parameters of the switching process are easily affected by the degree of aging. So the aging degree of IGBT can be calibrated by changes in its intrinsic characteristics, which can be represented by relevant aging parameters (turn-off delay time, turn-on delay time, Miller platform time).

(2) In the normal working environment of IGBT, the gate oxide layer aging process is a gradual aging process with time.

(3) Although the reliable detection of IGBT in the third stage is complex, it is of great significance. In the future, we can determine its residual life by detecting its degree of aging. Major accidents can be avoided by taking out and replacing the power devices before they are damaged.

ACKNOWLEDGMENT

The authors would like to thank the support of the On/off data of IGBT devices from Fanggang Sun in College of Electrical and Mechanical Engineering and Automation, Shanghai University.

REFERENCES

[1] G. Tang, H. Pang, and Z. He, "Development and application of advanced AC/DC power transmission technology in China," *Proc. CSEE*, vol. 36, no. 7, pp. 1760–1771, 2016.

[2] M. Wang, X. Zong, Y. Yuan, S. Liu, and K. Qian, "Reliability analysis of power generation system with photovoltaic power station," *Proc. CSEE*, vol. 33, no. 34, pp. 42–49, 2013.

[3] C. Busca, R. Teodorescu, F. Blaabjerg, S. Munk-Nielsen, L. Helle, T. Abeyasekera, and P. Rodriguez, "An overview of the reliability prediction related aspects of high power IGBTs in wind power applications," *Microelectron. Rel.*, vol. 51, nos. 9–11, pp. 1903–1907, Sep. 2011.

[4] C. Wang, Z. Wang, L. Zhang, D. Cao, and D. G. Dorrell, "A vehicle rollover evaluation system based on enabling state and parameter estimation," *IEEE Trans. Ind. Informat.*, early access, Jul. 27, 2020, doi: 10.1109/TII.2020.3012003.

[5] X. Ding, Z. Wang, L. Zhang, and C. Wang, "Longitudinal vehicle speed estimation for four-wheel-independently-actuated electric vehicles based on multi-sensor fusion," *IEEE Trans. Veh. Technol.*, vol. 69, no. 11, pp. 12797–12806, Nov. 2020, doi: 10.1109/TVT.2020.3026106.

[6] X. Yu, "Failure study of IGBT power module and bonding line state monitoring," Tianjin Univ. Technol., Tianjin, China, 2015.

[7] L. Ren, H. Wei, and C. Y. Gong, "Overview of fault characteristic parameters extraction technology of power electronic circuit power devices," *Proc. CSEE*, vol. 12, no. 35, pp. 3089–3101, 2015.

[8] H. Oh, B. Han, P. McCluskey, C. Han, and B. D. Youn, "Physics-of-failure, condition monitoring, and prognostics of insulated gate bipolar transistor modules: A review," *IEEE Trans. Power Electron.*, vol. 30, no. 5, pp. 2413–2426, May 2015.

[9] H. Z. Luo, "Research on the principle and method of on-line temperature extraction of large volume IGBT module based on dynamic thermistor method," Zhejiang Univ., Hangzhou, China, 2015.

[10] N. Baker, S. Munk-Nielsen, M. Liserre, and F. Iannuzzo, "Online junction temperature measurement via internal gate resistance during turn-on," in *Proc. 16th Eur. Conf. Power Electron. Appl.*, Lappeenranta, Finland, Aug. 2014, pp. 1–10, doi: 10.1109/EPE.2014.6911024.

[11] L. Shao, Y. Hu, and G. Xu, "A high precision on-line detection method for IGBT junction temperature based on stepwise regression algorithm," *IEEE Access*, vol. 8, pp. 186172–186180, 2020, doi: 10.1109/ACCESS.2020.3028904.

[12] Y.-S. Kim and S.-K. Sul, "On-line estimation of IGBT junction temperature using on-state voltage drop," in *Proc. Conf. Rec. IEEE Ind. Appl. Conf.*, Sep. 1998, pp. 853–859, doi: 10.1109/IAS.1998.730245.

[13] Y. Tang, B. L. Liu, and D. Z. Liu, "Threshold voltage reliability model based on IGBT gate fatigue mechanism," *power Electron.*, vol. 4, no. 49, pp. 36–38, 2015.

[14] P. V. Chen, "On-line monitoring of the MOSFET device junction temperature by computation of the threshold voltage," in *Proc. 3rd IET Int. Conf. Power Electron., Mach. Drives*, Dublin, Ireland, 2006, pp. 440–444.

[15] A. Ammous, B. Allard, and H. Morel, "Transient temperature measurements and modeling of IGBT's under short circuit," *IEEE Trans. Power Electron.*, vol. 13, no. 1, pp. 12–25, Jan. 1998.

[16] Z. Xu, F. Xu, and F. Wang, "Junction temperature measurement of IGBTs using short-circuit current as a temperature-sensitive electrical parameter for converter prototype evaluation," *IEEE Trans. Ind. Electron.*, vol. 62, no. 6, pp. 3419–3429, Jun. 2015.

[17] U. R. Vemulapati, E. Bianda, D. Torresin, M. Arnold, and F. Agostini, "A method to extract the accurate junction temperature of an IGCT during conduction using gate–cathode voltage," *IEEE Trans. Power Electron.*, vol. 31, no. 8, pp. 5900–5905, Aug. 2016.

[18] V. Smet, F. Forest, J.-J. Huselstein, A. Rashed, and F. Richardeau, "Evaluation of V_{ce} monitoring as a real-time method to estimate aging of bond wire-IGBT modules stressed by power cycling," *IEEE Trans. Ind. Electron.*, vol. 60, no. 7, pp. 2760–2770, Jul. 2013.

[19] A. S. Bahman, F. Iannuzzo, C. Uhrenfeldt, F. Blaabjerg, and S. Munk-Nielsen, "Modeling of short-circuit-related thermal stress in aged IGBT modules," *IEEE Trans. Ind. Appl.*, vol. 53, no. 5, pp. 4788–4795, Sep. 2017, doi: 10.1109/TIA.2017.2702594.

[20] Z. Wang, B. Tian, W. Qiao, and L. Qu, "Real-time aging monitoring for IGBT modules using case temperature," *IEEE Trans. Ind. Electron.*, vol. 63, no. 2, pp. 1168–1178, Feb. 2016, doi: 10.1109/TIE.2015.2497665.

[21] J. Liu, G. Zhang, Q. Chen, L. Qi, Y. Geng, and J. Wang, "*In situ* condition monitoring of IGBTs based on the miller plateau duration," *IEEE Trans. Power Electron.*, vol. 34, no. 1, pp. 769–782, Jan. 2019, doi: 10.1109/TPEL.2018.2820700.

[22] N. M. Vichare and M. G. Pecht, "Prognostics and health management of electronics," *IEEE Trans. Compon. Packag. Technol.*, vol. 29, no. 1, pp. 222–229, Mar. 2006, doi: 10.1109/TCAPT.2006.870387.

[23] B. Ji, V. Pickert, W. Cao, and B. Zahawi, "*In situ* diagnostics and prognostics of wire bonding faults in IGBT modules for electric vehicle drives," *IEEE Trans. Power Electron.*, vol. 28, no. 12, pp. 5568–5577, Dec. 2013.
[24] H. Huang and P. A. Mawby, "A lifetime estimation technique for voltage source inverters," *IEEE Trans. Power Electron.*, vol. 28, no. 8, pp. 4113–4119, Aug. 2013.
[25] H. Luo, Y. Chen, P. Sun, W. Li, and X. He, "Junction temperature extraction approach with turn-off delay time for high-voltage high-power IGBT modules," *IEEE Trans. Power Electron.*, vol. 31, no. 7, pp. 5122–5132, Jul. 2016.
[26] T.-Y. Hung, L.-L. Liao, C. C. Wang, W. H. Chi, and K.-N. Chiang, "Life prediction of high-cycle fatigue in aluminum bonding wires under power cycling test," *IEEE Trans. Device Mater. Rel.*, vol. 14, no. 1, pp. 484–492, Mar. 2014.
[27] Y.-H. Mei, J.-Y. Lian, X. Chen, G. Chen, X. Li, and G.-Q. Lu, "Thermo-mechanical reliability of double-sided IGBT assembly bonded by sintered nanosilver," *IEEE Trans. Device Mater. Rel.*, vol. 14, no. 1, pp. 194–202, Mar. 2014.
[28] L. Yang, P. A. Agyakwa, and C. M. Johnson, "Physics-of-failure lifetime prediction models for wire bond interconnects in power electronic modules," *IEEE Trans. Device Mater. Rel.*, vol. 13, no. 1, pp. 9–17, Mar. 2013.
[29] M. T. Quddus, T. A. DeMassa, and J. J. Sanchez, "Unified model for QBD prediction for thin gate oxide MOS devices with constant voltage and current stress," *Microelectron. Eng.*, vols. 51–52, pp. 357–372, May 2000.
[30] G. Groeseneken, R. Degraeve, T. Nigam, G. Van Den Bosch, and H. E. Maes, "Hot carrier degradation and time-dependent dielectric breakdown in oxides," *Microelectron. Eng.*, vol. 49, nos. 1–2, pp. 27–40, Nov. 1999.
[31] Y. Zhang, "Study on fatigue failure and aging characteristic parameters of IGBT power module," Shanghai Univ., Shanghai, China, 2020.
[32] W. Lai, M. Chen, L. Ran, S. Xu, N. Jiang, X. Wang, O. Alatise, and P. Mawby, "Experimental investigation on the effects of narrow junction temperature cycles on die-attach solder layer in an IGBT module," *IEEE Trans. Power Electron.*, vol. 32, no. 2, pp. 1431–1441, Feb. 2017.
[33] M. Y. Chen, B. Gao, and F. Yang, "Study on the health state of IGBT solder layer based on electrothermal-mechanical stress multi-physical field," *Trans. China Electrotechnical Soc.*, vol. 30, no. 20, pp. 252–260, 2015.
[34] N. Jiang, M. Y. Chen, S. Y. Xu, W. Lai, and B. Gao, "Thermal fatigue failure analysis of IGBT module with crack damage included," *J. Zhejiang Univ.*, vol. 51, no. 4, pp. 825–833, 2017.
[35] Y. Chen, "Study on the effects of the small swing of junction temperature cycles on solder layer in an IGBT module," in *Proc. Power Electron. Motion Control Conf.*, 2016, pp. 3236–3240.

GUOQING XU (Senior Member, IEEE) received the B.Sc., M.Sc., and Ph.D. degrees from Zhejiang University, Hangzhou, China, in 1988, 1991, and 1994, respectively, all in electrical engineering. In 1997, he joined Tongji University, Shanghai, China, where he was a Professor with the Department of Electrical Engineering, from 2000 to 2016. Since 2007, he has been a Research Professor and the Director of the CAS-CUHK Shenzhen Institute of Advanced Integration Technology, The Chinese University of Hong Kong. Since 2016, he has been the Chief Scientist of the Center for Automotive Electronics, Shenzhen Institutes of Advanced Technology, CAS. He is currently a Professor and the Director of the Institute of Electrical and Control Engineering, Shanghai University. His research interests include electric vehicle control, motor drive and energy processing, and automotive electronics.

LINGFENG SHAO received the B.S. degree in photoelectric information science and engineering from the Zhejiang University of Technology, Zhejiang, China, in 2017, and the M.S. degree from the Shanghai University of Electric Power, Shanghai, China, in 2020. He is currently pursuing the Ph.D. degree in electrical engineering with Shanghai University. His research interests include power electronic reliability, energy processing, and automotive electronics.

WEIWEI WEI was born in Anhui, China, in 1994. He received the M.S. degree from the Anhui University of Technology, Anhui, in 2019. He is currently pursuing the Ph.D. degree in electrical engineering with Shanghai University.

His research interests include physics-of-failure, condition monitoring, prognosis of power semiconductor devices and power equipment, high power density switching power supply, and new type power semiconductor device

YANHUI ZHANG received Ph.D. degree from the Guangzhou Institute of Energy Conversion, Chinese Academy of Sciences, in 2014. In 2014, he joined the Shenzhen Advanced Technology Research Institute, where he was mainly engaged in the research of battery management systems, industrial energy-saving optimization, and ocean engineering equipment.

XUECHENG SUN graduated from the State Key Laboratory of Micro and Nano Processing, Shanghai Jiao Tong University, in November 2017, and received the Ph.D. degree in electronic science and technology. In November 2019, he graduated from the National University of Singapore, as a Postdoctoral Fellow. He is currently working with the Microelectronics Research and Development Center, School of Computer Science and Engineering, Shanghai University, as the Deputy Director and a Master Supervisor, and an external expert of a research institute of China Aerospace Science and Industry Corporation. He has published 26 SCI articles in the sensor field and nine articles as the first author, including one in the *Cell* sub-journal. His research interests include magnetic sensor integrated detection chip, micro-nano processing technology, and magnetic biosensors. He is also a reviewer of more than 12 SCI journals, including *Nano Energy* (IF=15.58).